PREDICTED INFECTION RISK FOR AEROSOL TRANSMISSION OF SARS-COV-2

Martin Kriegel[1], Udo Buchholz[2], Petra Gastmeier[3], Peter Bischoff[3], Inas Abdelgawad[4], Anne Hartmann[1]

[1] Technical University of Berlin, Hermann-Rietschel-Institut

[2] Robert-Koch-Institute, Department for Infectious Disease Epidemiology

[3]Charité-University Medicine Berlin, Institute for Hygiene and Environmental Medicine

[4] Public Health Department Berlin Spandau

Address for correspondence:

Prof. Dr.-Ing. Martin Kriegel

Hermann-Rietschel-Institut

TU Berlin

m.kriegel@tu-berlin.de

Author contributions:

MK extended the existing models and performed the calculation. UB and IA supplied the data for retrospective analysis to validate the model. PG, PB, UB and IA evaluated the results from a medical point of view. AH performed the literature research and the review of the models and calculations. MK and AH drafted the manuscript. All authors contributed to the interpretation of the results, critically revised the paper and agreed on the final version for submission.

Abstract

Currently, the respiratory route is seen as the most important transmission path for SARS-CoV-2. In this investigation, models of other researchers which had the aim of predicting an infection risk for exposed persons in a room through aerosols emitted by an infectious case-patient were extended. As a novelty – usually neglected – parameters or boundary conditions, namely the non-stationarity of aerosols and the half-life of the aerosolized virus, were included and a new method for determining the quanta emission rate based on measurements of the particle emission rate and respiratory rate at different types of activities was implemented.

As a second step, the model was applied to twelve outbreaks to compare the predicted infection risk with the observed attack rate. To estimate a "credible interval" of the predicted infection risk, the quanta emission rate, the respiratory rate as well as the air volume flow were varied.

In nine out of twelve outbreaks, the calculated predicted infection risk via aerosols was found to be in the range of the attack rate (with the variation of the boundary conditions) and reasons for the observed larger divergence were discussed.

The validation was considered successful and therefore the use of the model could be recommended to predict the risk of an infection via aerosols in given situations. Furthermore, appropriate preventive measures can be designed.

Introduction

The respiratory route is the main mode of transmission for the virus causing COVID-19 (SARS-CoV-2) [1, 2, 3]. The virus is transported on particles that can enter the respiratory tract. Whereas larger particles (droplets) are only able to stay in the air for a short time and just in the near field (approx. 1.5 m), due to rapid settling, smaller particles (called aerosols) are also concentrated in the near field and in addition can follow the air flow and cause

infections in the far field. Epidemiologically, short-range transmission (through aerosols or droplets) is distinguished from long-range transmission (aerosol).

In order to perform an infection risk assessment for the airborne transmission in the far field and to introduce appropriate preventive measures, it would be necessary to know the amount of aerosols produced by an infected person during various activities, how many viruses stick to the aerosols and how many viruses are necessary to cause an infection. However, this information is usually available only very late in the course of a pandemic, if it can be determined at all. Another well-known approach is to use retrospective analysis of infection outbreaks that are very probably due to far field transmission to determine a virus-laden aerosol concentration. Exposed people have inhaled the virus-laden aerosols according to their respiratory volume flow. The approach presented here corresponds to a combination of known measured source rates of respiratory aerosols at different activities and the retrospective analysis of previous infection incidents with the aim to calculate a predicted infection risk via aerosols and to calculate the necessary air volume flow to reduce the risk of COVID-19 infections.

Current state

The so-called aerosols (liquid or solid particles in a dispersed phase with a fluid) as well as droplets differ by size. The particles, which are transported in a fluid over a longer distance, are called aerosols. Droplets are more strongly influenced by gravitation and are deposited more rapidly. The size of particles which can be transported in air for a longer distance varies with the velocity of the fluid. In internal spaces with typical air velocities of up to 0.2 m/s particles smaller than 10 µm will be distributed by air very well; with a higher air velocity, larger particles may also be transported in air.

SARS-CoV-2 was found to be transmitted via close contact as well as over distance in internal spaces, whereas in distant transmission so-called super-spreading events are more probable [1, 2, 4].

In 1978, Riley et al. [5] evaluated a measles outbreak in a suburban elementary school. Based on the number of susceptible persons (S), which have been infected (D) during each stage of infection, the risk (P) for an infection in this stage has been calculated with equation (1). Therefore, the risk for an infection has been defined as the percentage of infected persons from the number of pupils not already infected or vaccinated.

$$P = \frac{D}{S} \tag{1}$$

A Poisson-distribution of the risk of infection has been assumed as well as a stationary and evenly distributed concentration of the pathogens in the room air. Equation (2) shows the Poisson-distribution.

$$P = 1 - e^{-\lambda} \tag{2}$$

Therefore, Wells defined in 1955 [6] a size called quantum as the number of emitted infectious units, where the probability to get infected is $1 - e^{-1} = 63.2\%$. Hence, a quantum can be seen as a combination of the number of emitted aerosols with the virus transported on them and a critical dose which may result in an infection in 63.2 % of the exposed persons. Riley [5] combined the quantum concept with equation (2) to produce equation (3).

$$P = 1 - e^{-I \cdot q \cdot Q_b \cdot t/Q} \tag{3}$$

In equation (3), the number of infectious persons (I), the quanta emission rate depending on the activity (q), the pulmonary ventilation rate of exposed susceptible persons (Q_b), the duration of stay (t) and the volume flow of pathogen free air (Q) was used. The quotient q/Q represents the quanta concentration.

In poorly ventilated rooms, the assumption of a stationary concentration of quanta is not justified, because of the amount of time necessary before a stationary concentration is

reached. The normalized time-dependent concentration process can be calculated according to equation (4) and is shown in Figure 1. How rapidly the concentration of a human emitted contamination in a room raises depends on the air exchange rate (ACH) and the time (t). This relative concentration (c_{rel}) can be seen as an increase in the concentration compared to the volume flow.

$$c_{rel} = 1 - e^{-ACH \cdot t} \tag{4}$$

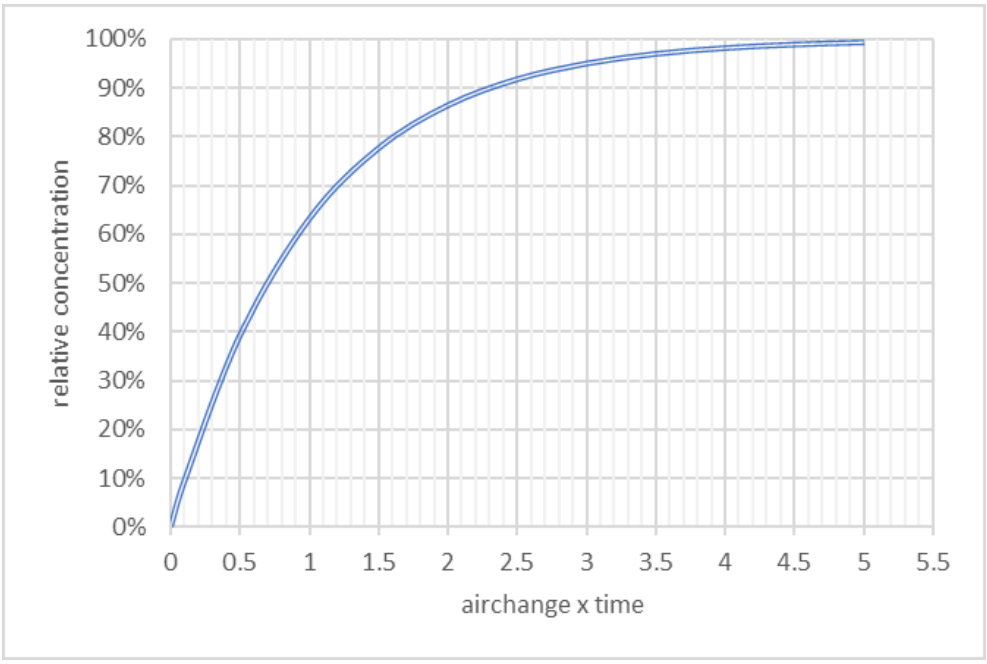

Figure 1: Relative concentration curve as a function of air exchange rate and time.

In all published studies identified, ideal mixing ventilation was assumed, which means that aerosols are evenly distributed in the room air. To avoid this assumption Noakes and Sleigh [7] divided the room air into different zones, which are themselves considered to be well mixed and have a uniform concentration. This should make it possible to calculate local differences in concentration and thus locally differing infection risks. Furthermore, other studies, which focus on the unsteady conditions mostly use the boundary condition of a starting concentration of $c(t = 0) = 0 \frac{quanta}{m^3}$. Gammaitoni and Nucci [8] implemented the

89 starting condition of $c(t = 0) = c_0$ as well as the number of exposed susceptible people,
90 which may also change over time depending on their immune status.
91
92 To estimate the risk of infection in a given setting by a given infectious person with the
93 Wells-Riley-equation either the quanta emission rate or the P have to be known. In the
94 beginning of an epidemic, both values are unknown. Dai and Zhao [9] correlated and
95 calculated q for SARS-CoV-2 based on the basic reproduction number (R_0) known from
96 former outbreaks of MERS, tuberculosis, influenza and SARS-CoV-1 and published the
97 equation (5). If R_0 is known, q can be estimated as proposed by Dai and Zhao [9]. For SARS-
98 CoV-2 the average basic reproduction number has been estimated to be 3.28 [10], 3.32 [11]
99 and 3.77 [12].

$$q = -30.27958 - 44.81536 \cdot R_0 + 19.67934 \cdot R_0^2 \quad (5)$$

100
101 In various studies of infection occurrences associated with SARS-CoV-2, q was determined
102 using the Wells-Riley equation. Different authors [9, 13] found a range of 22 to 61 quanta/h
103 with an assumed low activity (breathing, speaking) and values of 341 to 1190 quanta/h when
104 singing.
105
106 The virus can be transported on particles in air and the emission of aerosols can be used as an
107 indicator for the emission of the virus, but a correlation between q and the aerosol emission
108 rate (E) has not been investigated so far. In measurements at the Hermann-Rietschel-Institute
109 (HRI) of Technical University of Berlin [14, 15] the particle emission rates during breathing,
110 speaking, coughing as well as singing was measured. During breathing through the nose about
111 25 particles/s was emitted and during coughing about 13,700 particles/cough. It is therefore
112 evident that depending on the activity a wide range of particle emission rates can be found.

113 The transmission of a pathogen via aerosols is also influenced by the stability of the virus in
114 the environment. In an experimental study van Doremalen et al [16] measured the decrease of
115 infectious virus in the air and on different surfaces and compared SARS-CoV-1 and SARS-
116 CoV-2. Under the given conditions, the half-life of SARS-CoV-2 as well as SARS-CoV-1
117 was about 1.1 h.
118 The longer aerosols stay in the room air, the more the proportion of inactivated virus
119 increases. The age of air is dependent on the airflow as well as the position of the source of
120 the pollutants. At each point in the room, a local age of air can be calculated. The age of air
121 (τ_n) can be used as a measure to evaluate the air quality. For an ideal mixing ventilation, the
122 mean age of air is equal to the nominal time constant, which can be calculated using equation
123 (6) as the quotient of the room volume (V) and the air volume flow (Q).

$$\tau_n = \frac{V}{Q} \tag{6}$$

124 Besides the number of emitted pathogen-laden aerosols, the number of inhaled pathogens also
125 plays an important role, with regard to the assessment of the risk of infection. The pulmonary
126 ventilation rate may differ with different activities. Gupta et al. [17] performed a study with
127 25 healthy adults and found that the volume flow fluctuated in the form of a sine wave during
128 simple breathing, but gave a more constant volume flow during talking.
129 In measurements with athletes as well as sedentary persons a maximum volume flow for the
130 athletes of 200 l/min (12 m^3/h) was found by Córdova and Latasa [18].
131 To measure the airflow without movement restrictions, a helmet was used by Jiang et al. [19]
132 in 32 subjects (16 males, 16 females) during speaking with different volumes as well as
133 during singing.
134 A comparison between a machine-learning based model and measurements of respiratory rate
135 was performed by Dumond et al. [20].
136 As a conclusion, the following average values can be used for adults:

- low activity (breathing while lying): 0.45 m^3/h [19]
- low activity (breathing while sitting, standing or talking): 0.54 m^3/h [19, 20]
- singing: 0.65 m^3/h [21]
- mid activity (physical work): 0.9 m^3/h [20]
- sports: 1.2 m^3/h [18, 20]

For children, the lung volume is smaller. Therefore, the respiratory rate for children aged 14 can be assumed to be 0.45 m^3/h for low activity (breathing while sitting, standing, talking) [22].

Methods

Extension of the Wells-Riley equation for calculating the Predicted Infection Risk via Aerosols (PIRA)

The Wells-Riley equation can be summarized as equation (7). To calculate the predicted infection risk via aerosols (PIRA) in the far field of a room the concentration of quanta (c(t)) and the respiratory rate (Q_b) must be known. The integration of c(t) can be understood as the number of particles inhaled per m^3/h. Together with Q_b, the number of inhaled quanta can therefore be calculated.

$$PIRA = 1 - e^{(-\int[c(t)]\cdot Q_b)} \quad (7)$$

Equation (5) can be used for the definition of the quantum emission. This leads to a quanta emission rate of q = 40 1/h at an assumed mean R_0 = 3.35. The mathematical approximation presented by Dai und Zhao [9] can be optimized by equation (8), see Figure 2. For Figure 2 the quanta emission rate has been correlated with R_0 of tuberculosis [23, 24], Influenza [23, 25], MERS [26, 27] and SARS-CoV [23, 28].

159 Equation (8) results in q = 139 1/h for an assumed mean R_0 = 3.35. Because of the high
160 variance of the q as well as R_0 given in the currently available literature the difference
161 between the q calculated regarding equation (5) and equation (8) seems reasonable.

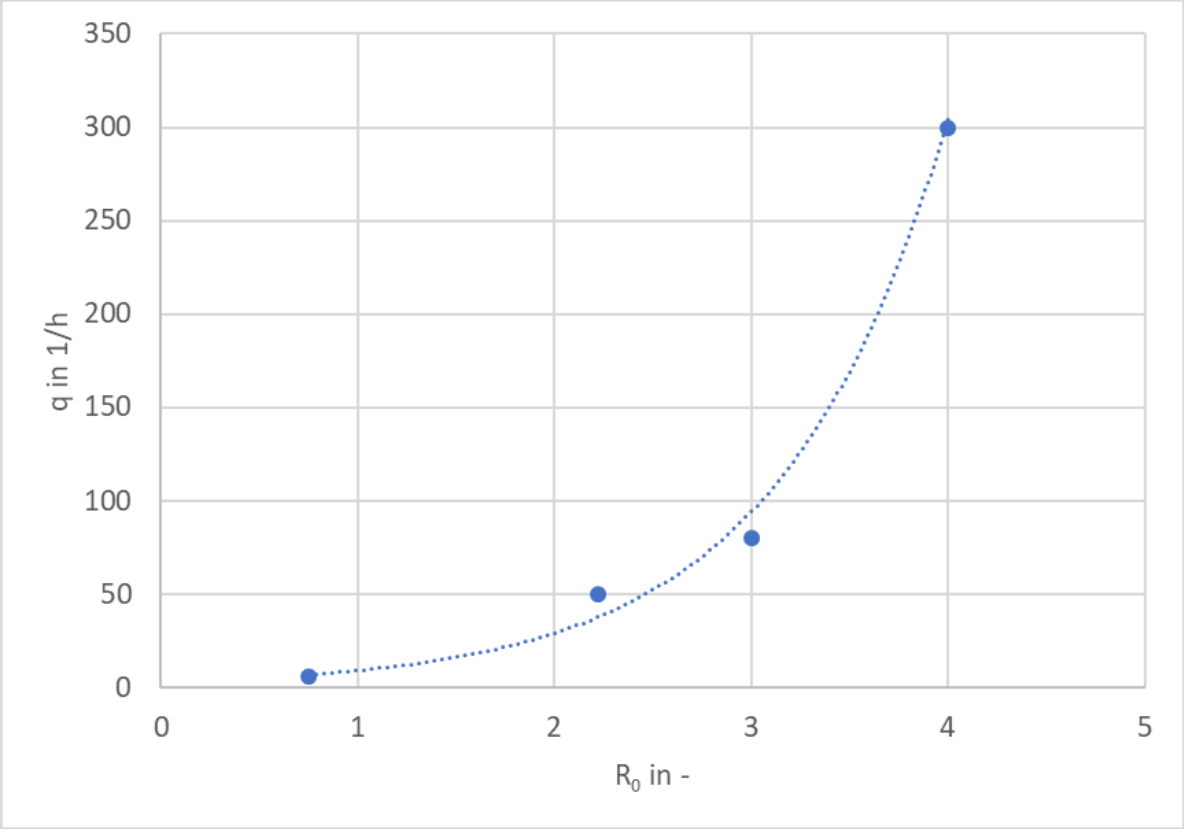

162 *Figure 2: Relationship between quanta emission rate and R_0 according Dai and Zhao* [9]

163

$$q_0 = 2.7618 \cdot (e^{1.1761 \cdot R_0} - 1) \quad (8)$$

164

165 q is influenced by the activity of the person as was shown by Buonanno et al. [29]. Therefore,
166 the measured aerosol emission rates E [14, 15] were correlated with the calculated quanta
167 emission rates influenced by the activity q_a by equation (9). For low-activity (breathing,
168 talking, sitting, standing) a basic volume flow $Q_{b,o}$ and normal activity = low activity
169 (breathing, talking, sitting, standing) with a basic emission rate of E_0 was used. Furthermore,
170 the basic q (q_0) was calculated with usage of R_0 regarding equation (8). With these
171 specifications q_a can be calculated.

$$q_a = q_0 \cdot \frac{E}{E_0} \cdot \frac{Q_b}{Q_{b,0}} \tag{9}$$

$$Q_{b,0} = 0.54 \frac{m^3}{h}; \qquad E_0 = 100 \frac{P}{s} [15]$$

172

173 The effect of e.g. mouth-nose protection can be considered by using their filtration efficiency
174 (F_{MNS}) like in equation (10) which however will not be further considered in the following.

$$q_{a,MNS} = F_{MNS} \cdot q_a \tag{10}$$

175

176 It is known that the infectivity of an infected person depends on the disease progression over
177 time [30]. This is shown qualitatively in Figure 3. With a simplified mathematical approach,
178 this can be integrated into the quanta source rate. An equation could be implemented to take
179 this into account.

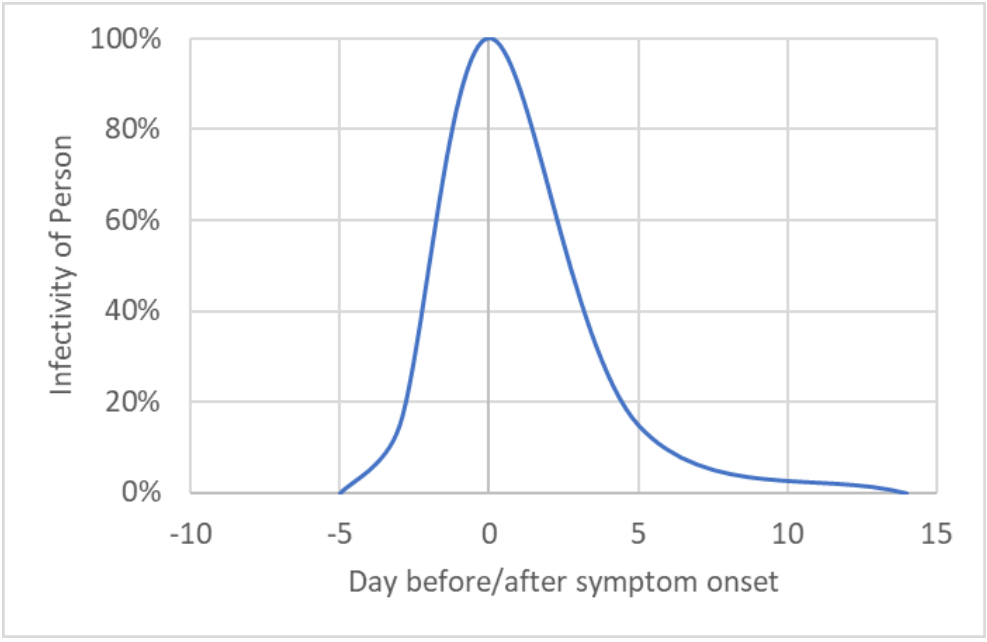

180

181 *Figure 3: Infectivity depending on the disease progression*

182

183 Under experimental conditions, the half-life of virus was measured as 1.1 h [16]. Thus, the
184 number of emitted infectious quanta at time t ($q_a(t)$) is calculated according to equation (11).

$$q_a(t) = q_a \cdot e^{(-0.5776 \cdot t)} = q_a \cdot e^{\left(-\frac{361}{625} \cdot t\right)} \tag{11}$$

185 The concentration of quanta during the increase $c_I(t)$ can be calculated according to equation
186 (12) with the number of infectious persons (n).

$$c_I(t) = \frac{q_a(t)}{Q} \cdot n \cdot \left(1 - e^{(-ACH \cdot t)}\right) \tag{12}$$

187 An additional case is considered that if the time t is longer than the age of the air τ_n, most of
188 the virus-laden aerosols have left the room with the exhaust before the inactivation can take
189 place. Therefore, this concentration during the steady state situation is called $c_\tau(t)$.

$$q_{a,\tau} = q_a \cdot e^{(-0.5776 \cdot \tau_n)} \tag{13}$$

$$c_\tau(t) = \frac{q_{a,\tau}}{Q} \cdot n \cdot \left(1 - e^{(-ACH \cdot t)}\right) \tag{14}$$

190 with τ_n regarding equation (6)

191

192 For calculating the risk of infection the unsteady concentrations c_I and c_τ has to be used, to
193 include the time-dependent increase in concentration and to include the time-dependent
194 viability of the virus, otherwise the result could be overestimated or underestimated.
195 For equation (7) the integration of $c_I(t)$ and $c_\tau(t)$ is necessary.

$$C_I = \int_0^t c_I(t) = \frac{q_a \cdot \left(390625 \cdot ACH - \left((390625 \cdot ACH + 225625) \cdot e^{ACH \cdot t} - 225625\right) \cdot e^{-ACH \cdot t - \frac{361}{625} \cdot t}\right)}{Q \cdot (225625 \cdot ACH + 130321)} \tag{15}$$

$$C_\tau = \int_\tau^{t \geq \tau_n} c_\tau(t) = \frac{q_{a,\tau} \cdot e^{-ACH \cdot (t+\tau_n)} \cdot \left(ACH \cdot (t - \tau_n) \cdot e^{ACH \cdot (t+\tau_n)} - e^{ACH \cdot t} + e^{ACH \cdot \tau_n}\right)}{Q \cdot ACH} \tag{16}$$

196

197 The Predicted Infection Risk via Aerosols can be calculated by equation (17) and (18).

$$PIRA = 1 - e^{(-(C_I(t=\tau) + C_\tau) \cdot Q_b)} \qquad t > \tau_n \tag{17}$$

$$PIRA = 1 - e^{(-(C_I)\cdot Q_b)} \qquad t \leq \tau_n \tag{18}$$

198

199 For the calculation of PIRA the following assumptions must be considered:

200 • the aerosols are ideally mixed in the room

201 • the near field (up to approx. 1.5 m distance from the emitting person) can contain a
202 much higher virus-laden aerosol concentration

203 • the air, which is introduced into the room, is free of virus-laden aerosols (e.g. outside
204 air)

205 • no deposition of small particles is considered, because the settling time is longer than
206 the stability of the virus and the deposition rate would therefore be substantially
207 smaller than the inactivation

208 • the concentration of aerosols at the beginning is 0

209 **Results**

210 The PIRA calculation model was validated by using parameters of several known outbreaks
211 during the SARS-CoV-2 pandemic. Twelve different scenarios either scientifically published
212 or registered by the local health authorities were selected (A-L). The boundary conditions for
213 the calculations of these situations can be found in Table 1.

Table 1: Boundary conditions of SARS-CoV-2 outbreaks for the retrospective calculation of PIRA

	A	B	C	D	E	F	G	H	I	J	K	L
V in m^3	3000	1200	60*	630	254	830	180	150	150	47	170	60***
n	1	1	1	1	1	1	1	1	1	1	1	1
q_a in 1/h	232	4213	139	139	139	4213	116	116	139	139	139	139
Q_b in m^3/h	0.9	0.65	0.54	0.54	0.54	0.65	0.45	0.45	0.54	0.54	0.54	0,54
Q in m^3/h	1600	200*	200*	4000**	50*	200*	1500*	1500*	400*	75	200*	1260***
exposure time t in h	8	2.5	1.66	8	1.5	2.5	4.5*****	1.5*****	4.5*****	1.2	2	11
Attack Rate**** in %	26%	91%	34%	5%	58%	87%	10%	6%	43%	45%	17%	63%

*due to partly missing information, assumptions were made, especially for window ventilation. The assumptions are based on information from the persons involved on how the windows were opened and closed in combination with weather data at the time.

** It was assumed that the local regulations for fresh air supply were fulfilled.

***Geometry and Ventilation Rate due to [31]

****Attack Rate was simplified as percentage of persons infected. No separation regarding infection attack rate (measured serologically) and illness attack rate (persons with symptoms or laboratory-confirmed) was performed.

***** It was assumed that a school lesson lasts 45 minutes.

	Setting	Country	Remarks
A	Slaughterhouse [32]	Germany	
B	Choir rehearsal Berlin	Germany	not yet scientifically published, investigated by Robert-Koch-Institute
C	Bus Tour [33]	China	
D	Call Center [34]	Korea	The attack rate is mentioned as 43 % in the publication. However, the infection occurred almost exclusively on one half of the 11th floor. The local attack rate is therefore actually significantly higher. In Table 1 an attack rate of 5% was given, because only persons who had shown symptoms were quarantined. If one includes the persons who showed symptoms up to and including 04.02., the attack rate is 5 %.
E	Club Meeting	Germany	not yet scientifically published, investigated by Robert-Koch-Institute
F	Choir rehearsal Skagiq [13]	USA	
G	School Berlin 1	Germany	not yet scientifically published, investigated by Public Health Department Berlin Spandau
H	School Berlin 2	Germany	not yet scientifically published, investigated by Public Health Department Berlin Spandau
I	School Israel [35]	Israel	
J	Restaurant [1, 36]	China	
K	Meeting	Germany	not yet scientifically published, investigated by Robert-Koch-Institute
L	Aircraft [37]	-	

215

The infection events used for the validation of the model are shown in Table 1 with the necessary parameters for the calculation. In the following, the comparison between the documented Attack Rate (AR) and the PIRA is drawn.

The q used here was calculated according to equation (9) with the assumption that the cases emitted particles as measured in [14, 15]. Due to the high spread of the particle emission E and the unknown proportions of breathing, speaking, singing and shouting as well as the respiratory volume flows, simplified a-priori assumptions were made. To take into account the effects of the uncertainties regarding q, Q_b and especially with window ventilation on Q, these values were further varied - q by +/- 20%, Q_b by +/- 20% and Q by +/- 50%, individually and in combination, which then lead to a minimum PIRA and maximum PIRA. Figure 4 presents PIRA and the minima and maxima calculated with the different variants. The red dots show the documented AR.

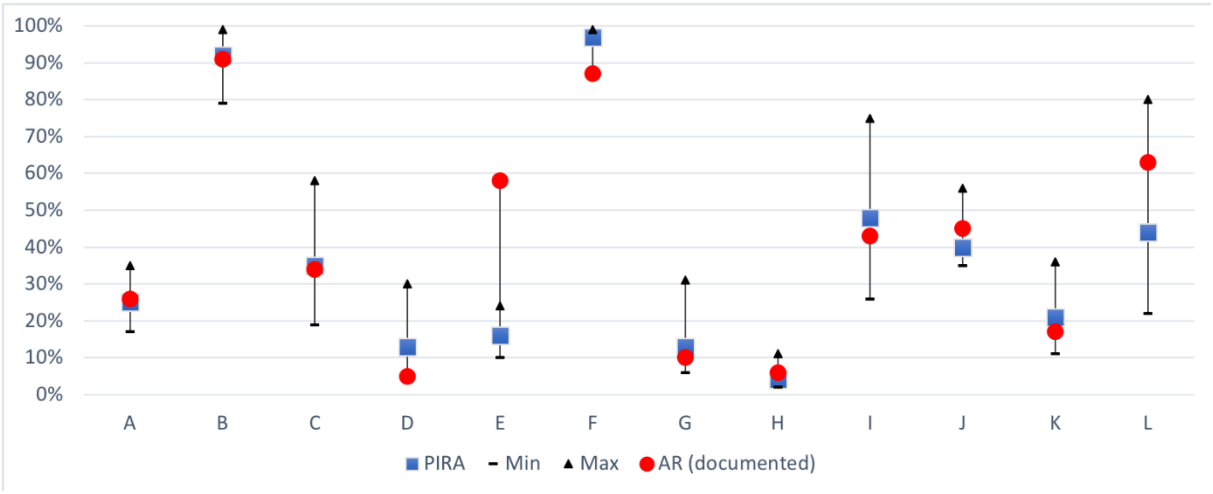

Figure 4: Comparison between PIRA with the variants Min and Max to the documented AR assuming that all cases were caused by long-range transmission

In nine out of twelve outbreaks, the attack rate lies in the Min Max values of the calculated PIRA (see Table 2).

Table 2: Results of the Calculation of PIRA and comparsion with the documented AR

	A	B	C	D	E	F	G	H	I	J	K	L
PIRA	25%	92%	35%	13%	16%	97%	13%	4%	48%	40%	21%	44%
Min	17%	79%	19%	6%	10%	88%	6%	2%	26%	35%	11%	22%
Max	35%	99%	58%	30%	24%	99%	31%	11%	75%	56%	36%	80%
AR (documented)	26%	91%	34%	5%	58%	87%	10%	6%	43%	45%	17%	63%

From the PIRA model, it can be calculated how much volume flow per hour of exposure time is required to not exceed a certain PIRA. The results are shown in Figure 5. It can be seen that for a PIRA of 10% a volume flow of clean air of 750 m³/h and hour of exposure has to be supplied to the room (see Table 3), whereas for two hours 1500 m³/h will be necessary for the same PIRA.

As a regression of the calculated results presented in Figure 5, equation (19) was derived. Using equation (19) the required volume flow per hour of exposure time can be calculated. This information refers to the steady state if the product of ACH and t is higher than 5.0, see Figure 1. If the product is smaller, correspondingly lower volume flows lead to the respective PIRA.

$$Q_{sp} = 75 \cdot \frac{1}{PIRA} \tag{19}$$

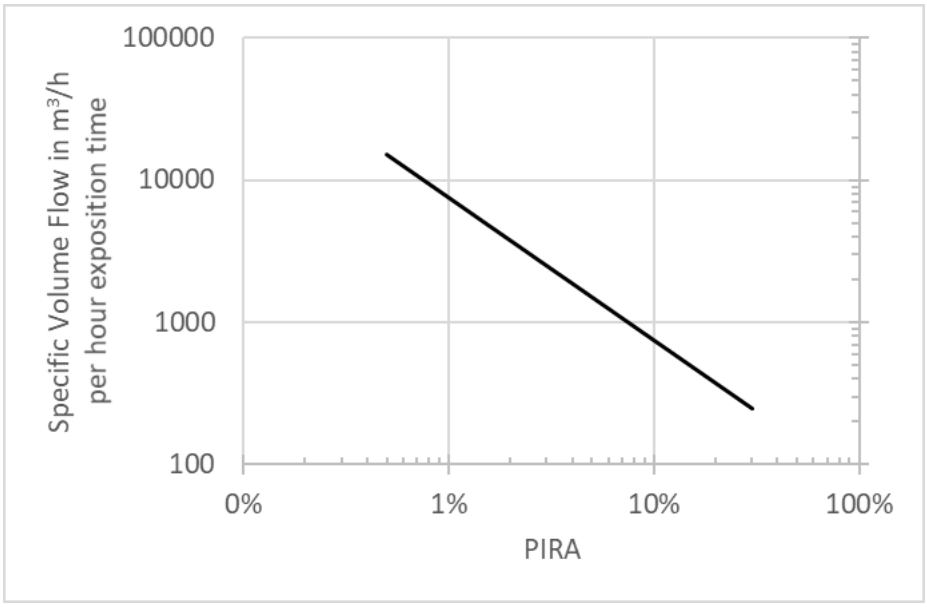

Figure 5: Required specific volume flow per hour exposure time with regard to meeting a specific PIRA

Table 3 lists practical examples of the required volume flows depending on the exposure time and PIRA.

Table 3: Required volume flow at a certain exposure time for a defined PIRA

		PIRA		
		1%	5%	10%
exposure time in h	1	7500 m^3/h	1500 m^3/h	750 m^3/h
	2	15000 m^3/h	3000 m^3/h	1500 m^3/h
	3	22500 m^3/h	4500 m^3/h	2250 m^3/h

Another type of evaluation shows the possible number of infected persons in relation to the person-related volume flow and the number of persons in a room (see Figure 6), if several exposed persons are in a room and each person would have 6 m^3 of room volume available. If more volume flow is available to each person, the result changes marginally and tends towards a lower PIRA. For an exposure time of two hours a volume flow of 20 m^3/(h·Per)

resulted in five probably infected persons in a room with 20, 40 or 100 persons, but of course only one probably infected person in a room with two persons. For a volume flow of 60 m³/(h·Per) the number decreases to two probably infected persons in a room with 20, 40 or 100 persons, but of course stayed at one probable person for just two persons in a room.

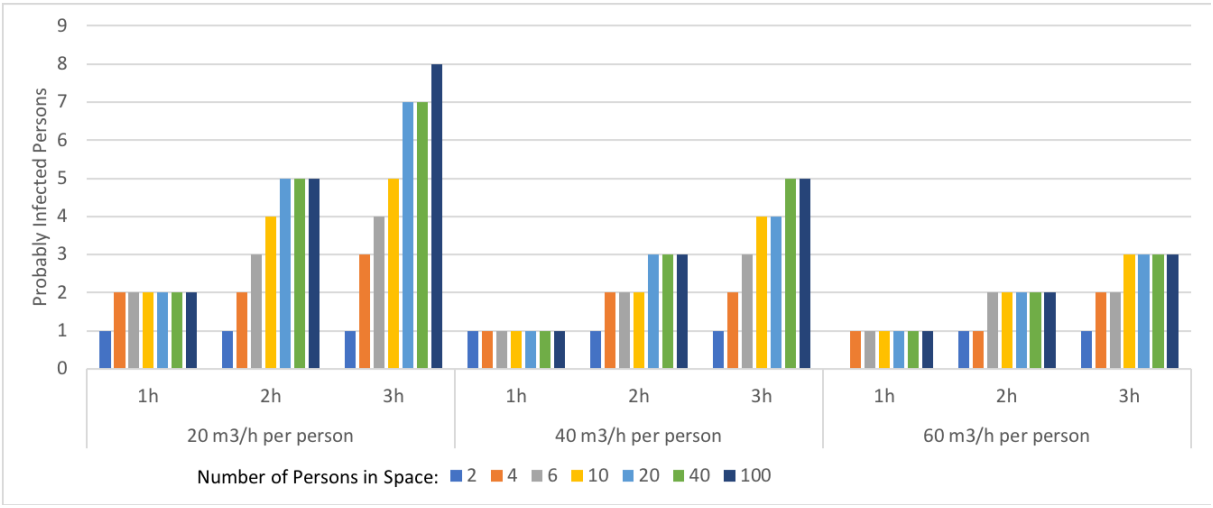

Figure 6: Number of persons probably infected according to a specific volume flow

Discussion

For the first time with a q based on R_0 the PIRA was calculated for different known SARS-CoV-2 outbreaks. In addition, the necessary air volume flows to reduce the risk of infection were calculated.

In Table 4 the q-values are compared according to the stationary equation (3) and the PIRA model under the boundary conditions of Table 1. Large differences between the same activities were observed in the calculation of the steady-state.

First of all, in comparison, with fixed q according to equation (9) very good agreement can be achieved with the documented AR in the retrospectively considered cases A, B, C, H, I, J, K.

Table 4: comparison steady state and unsteady calculated quanta

	q in 1/h											
	A	B	C	D	E	F	G	H	I	J	K	L
q steady state	255	344	275	965	67	449	808	2545	223	144	411	330
q unsteady	232	4213	139	139	139	4213	116	116	139	139	139	139

In outbreak D, the documentation does not clearly show how large the actual AR was for the area under consideration. Due to the fact, that only the person who showed symptoms was isolated, it is possible that in the meantime, additional persons, who were already infected by the index case may have infected others (e.g. pre-symptomatically) leading to the high AR.

In outbreak E, there is little documentation of the infection process, and further contact between some of the persons had occurred in a restaurant afterwards. Furthermore, it has not been determined whether the infection can be attributed to only one person. The high AR after a short time of exposure allows the conclusion that either two index persons were present or that the exposure time was prolonged by the meeting in a restaurant.

In outbreak F, the group was not together for the entire time and some of the subjects continued rehearsing in another room. For this reason, the exposure time for the whole group was lower and this may account for the lower AR than calculated by PIRA.

In outbreak L an air exchange rate of 21 1/h was assumed. A relatively small change in the assumed volume flow has a significant influence on the result of PIRA (where the total exposure time was used). Furthermore, it cannot be excluded that droplet transmission may also have happened.

Secondly, many assumptions were made, therefore it is not clear if the formula is already optimal, perhaps further optimization during the course of the pandemic is possible if further knowledge becomes available.

Third, the calculation model does not consider the sedimentation behavior of particles. It is known that at higher air velocities, and especially at high turbulence, the sedimentation behavior increases. In typical indoor air flows this decrease is about 10 % per hour. Compared to the uncertainty of the overall emission rate, this effect is not significant.

Fourth, the calculation model assumes a homogeneous distribution of the particles in the room air. Practically however, the ventilation effectiveness is locally very different. The differences can be slightly greater than 100%.

Finally, it must be noted that the aerosol concentration is significantly higher in the near field of the emitting person and the results of PIRA are not valid within the generally accepted 1.5 m distance rules.

Conclusion

It was shown in this investigation that it was possible to calculate the risk of an infection via aerosols for situations where the long-distance transmission is more important. By using the model presented here, a good agreement to previous infection outbreaks in different settings and different attack rates was achieved. Previous retrospectively determined quanta emission rates usually assumed a stationary state. However, if the concentration process is important for the total amount of inhaled virus-laden aerosols (usually at ACH x $t < 5$), then a stationary observation leads to an incorrect boundary condition. The time-dependent viability of the virus also plays a significant role. Here, the influence of the viability is higher at low air change rates compared with high ones, because the virus stays in the room air for a longer time period and the proportion of inactivated pathogens increase. However, the effect of time-dependent viability is not that important that a low air change rate has an overall positive effect.

To reduce the risk of infection via aerosols the necessary volume flow of virus-free air depending on the exposure time can be seen in Figure 5. This figure may be helpful to

implement measures, such as increasing the virus-free air supply rate. Furthermore, the number of exposed persons must be kept in mind. An infection risk of 60% may result in one infected person in a two-person office, but in 60 infected persons in a room with 100 persons.

Predicting the infection risk via aerosols and knowing the important parameters can help in the selection of appropriate preventive actions.

Acknowledgement

We thank Claudia Ruscher (State Office for Health and Social Affairs (LAGeSo), Berlin, Germany), Marius Hausner (Local Health Authority of Berlin-Mitte, Berlin, Germany), Mareike Kunze (Local Health Authority of Berlin-Mitte, Berlin, Germany), Bettina Weiss (Local Health Authority of Charlottenburg-Wilmersdorf, Berlin, Germany) and Felix Reichert (Department of infectious disease epidemiology, Robert Koch-Institute, Berlin, Germany) for providing information on outbreak B, as well as Sabine Timm (Bernau, Berlin) for providing information on outbreak K.

Declarations

The authors received no specific funding for this work.

The authors declare no competing interests.

The authors declare that they followed the appropriate research guidelines.

Literature

[1] Y. Li, H. Qian, J. Hang, X. Chen, L. Hong, P. Liang, J. Li, S. Xiao, J. Wie, L. Liu and M. Kang, "Evidence for probable aerosol transmission of SARS-CoV-2 in a poorly ventilated restaurant," *Preprint medXRiv,* 2020.

[2] G. Correia, L. Rodrigues, M. Gameiro da Silva and T. Gonçalves, "Airborne route and bad use of ventilation systems as non-neglible factors in SARS-CoV-2 transmission," *Medical Hypotheses,* vol. 141, 2020.

[3] L. Ferretti, C. Wymant, M. Kendall, L. Zhao, A. Nurtay, L. Abeler-Dörner, M. Parker, D. Bonsall and C. Fraser, "Quantifying SARS-CoV-2 transmission suggests epidemic control with digital contact tracing," *Science,* vol. eabb6936, p. 368, 2020.

[4] L. Morawska and J. Cao, "Airborne transmission of SARS-CoV-2: The world should face the reality," *Environment International,* vol. 139, 2020.

[5] E. Riley, G. Murphy and R. Riley, "Airborne Spread of Measles in a Suburban Elementary School," *American Journal of Epidemiology,* vol. 107, no. 5, pp. 421-432, 1978.

[6] W. Wells, Airborne contagion and air hygiene: an ecological study of droplet infections, 1955.

[7] C. Noakes and A. Sleigh, "Applying the Wells-Riley equation to the risk of airborne infection in hospital environments: The importance of stochastic and proximity effects," in *Indoor Air*, Copenhagen, Denmark, 2008.

[8] L. Gammaitoni and M. Nucci, "Using a Mathematical Model to Evaluate the Efficacy of TB Control Measures," *Emerging Infectious Diseases,* vol. 3, no. 3, pp. 335-342, 1997.

[9] H. Dai and B. Zhao, "Association of the infection probability of COVID-19 with ventilation rates in confined spaces," *Building Simulations,* 2020.

[10] y. Liu, G. AA., A. Wilder-Smith and J. Rocklöv, "The reproductive number of COVID-19 is hisher compared to SARS coronavirus," *Journal of Travel Medicine,* pp. 1-4, 2020.

[11] Y. Alimohamadi, M. Taghdir and M. Sepandi, "The Estimate of the Basic Reproduction Number of Novel Coronavirus disease (COVID-19): A Systematic Review and Meta-Analysis," *Journal of Preventive Medicine and Public Health,* vol. March, 2020.

[12] Y.-F. Lin, Q. Duan, Y. Zhou, T. Yuan, P. Li, T. Fitzpatrick, F. Leiwen, A. Feng, G. Luo, Y. Zhan, B. Liang, S. Fan, Y. Lu, B. Wang, Z. Wang, H. Zhao, Y. Gao, M. Li, D. Chen, X. Chen, Y. Ao, L. Li, W. D. X. Cai, Y. Shu and H. Zhou, "Spread and Impact of COVID-19 in China: A Systematic Review and Synthesis of Predictions From Transmission-Dynamic Models," *frontiers in Medicine,* 2020.

[13] S. Miller, W. Nazaroff, J. Jimenez, A. Boerstra, G. Buonanno, S. Dancer, J. Kurnitski, L. Marr, L. Morawska and C. Noakes, "Transmission of SARS-CoV-2 by inhalation of respiratory aerosol in the Skagit Valley Chorale superspreading event," *Preprint medXRiv,* 2020.

[14] D. Mürbe, M. Kriegel, J. Lange, H. Rotheudt and M. Fleischer, "Aerosol emission is inscreased in professional singing," *Preprint,* 2020.

[15] A. Hartmann, J. Lange, H. Rotheudt and M. Kriegel, "Emission rate and particle size of bioaerosols during breathing, speaking and coughing," *Preprint,* 2020.

[16] N. van Doremalen, T. Bushmaker, D. Morris, M. Holbrook, A. Gamble, B. Williamson, A. Tamin, J. T. N. Harcourt, S. Gerber, J. Lloyd-Smith, E. de Wit and V. Munster, "Aerosol and Surface Stability of SARS-CoV-2 as Compared with SARS-CoV-1," *New England Journal of Medicine,* Vols. April, 16, p. 382, 2020.

[17] J. Gupta, C.-H. Lin and Q. Chen, "Characterizing exhaled airflow from breathing and talking," *Indoor Air,* vol. 20, pp. 31-39, 2010.

[18] A. Córdova and I. Latasa, "Respiratory flows as a method for safely preventing the coronvirus transmission (COVID-19)," *Apunts Sports Medicine,* vol. 55, pp. 81-85, 2020.

[19] J. Jiang, R. Hanna, M. Willey and A. Rieves, "The measurement of airflow using Singing helmet that allows free movement of the jaw," *Journal of Voice,* vol. 30, no. 6, pp. 641-648, 2016.

[20] R. Dumond, S. Gastinger, H. Rahman, A. Le Faucheur, P. Quinton, H. Kang and J. Prioux, "Estimation of respiratory colume from thoracoabdominal breathing distances: comparison of two models of machine learning," *European Journal of Applied Physiology,* vol. 117, pp. 1533-1555, 2017.

[21] B. Binazzi, B. Lanini, R. Bianchi, I. Romagnoli, M. Nerini, F. Gigliotti, R. M.-E. J. Duranti and G. Scano, "Breathing Pattern and kinematics in normal subjects during speech, singing and loud whispering," *Acta Physiologica,* vol. 186, pp. 233-246, 2006.

[22] Spektrum Akademischer Verlag, Heidelberg, "Lexikon der Biologie," spektrum.de, 1999. [Online]. Available: https://www.spektrum.de/lexika/showpopup.php?lexikon_id=9&art_id=5744&nummer=1988. [Accessed 05 Oktober 2020].

[23] B. Stephens, "HVAC Filtration and the Wells-Riley approach to assessing risks of infectious airborne diseases," 2013.

[24] S.-C. Chen, C.-M. Liao, S.-S. Li and S.-H. You, "A Probabilistic Transmission Model to Assess Infection Risk from Mycobacterium Tuberculosis in Commercial Passenger Trains," *Risk Analysis,* vol. 31, no. 6, pp. 930-939, 2011.

[25] G. Chowell, H. Nishiura and L. M. A. Bettencourt, "Comparative estimation of the reproduction number of pandemic influenza from daily case notification data," *Journal of the Royal Society Interface,* vol. 4, pp. 155-166, 2006.

[26] B. J. Coburn and S. Blower, "Predicting the potential for within-flight transmission and global dissemination of MERS," *The Lancet,* no. 14, 2014.

[27] WHO, "WHO MERS Global Summary and Assessment of Risk," WHO, 2019.

[28] WHO, "Consensus document on the epidemiology of severe acute respiratory syndrome (SARS)," WHO, 2003.

[29] G. Buonanno, L. Stabile and L. Morawska, "Estimation of airborne viral transmission: Quanta emission rate of SARS-CoV-2 for infection risk assessment," *Environment International,* vol. 141, 2020.

[30] X. He, E. H. Y. Lau, P. Wu, X. Deng, J. Wang, X. Hao, Y. C. Lau, J. Y. Wong, Y. Guan, X. Tan, X. C. Y. Mo, B. Lio, W. Chen, F. Hu, Q. Zhang, M. Zhong, Y. Wu, L. Zhao, F. Zhang, C. B. J., F. Li and G. M. Leung, "Author Correction: Temporal Dynamics in viral shedding and transmissibilitiy of COVID-19," *Nature Medicine,* 2020.

[31] N. A. o. Sciences, The Airliner Cabin Environment and the Health of Passengers and Crew, United States of America: National Academy Press, 2002.

[32] T. Günther, M. Czech-Sioli, D. Indenbirken, A. Robitailles, P. Tenhaken, M. Exner, M. Ottinger, N. Fischer, A. Grundhoff and M. M. Brinkmann, "Investigation of a superspreading event preceding the largest meat processing plant-related SARS-Coronavirus 2 outbreak in Germany," *Preprint,* 2020.

[33] Y. Shen, C. Li, H. Dong, Z. Wang, L. Martinez, Z. Sun, A. Handel, Z. Chen, E. Chen, M. Ebel, F. Wang, B. Yi, H. Wang, X. Wang, A. Wang, B. Chen, Y. Qi, L. Liang, Y. Li, F. Ling, J. Chen and G. Xu, "Community Outbreak Investigation of SARS-CoV-2 Transmission Among Bus Riders in Eastern China," *JAMA International Medicine,* 2020.

[34] S. Park, Y.-M. Kim, S. Lee, B.-J. Na, C. Kim, J.-i. Kim, H. Kim, Y. Kim, Y. Park, I. Huh, H. Kim, H. Yoon, H. Jang, K. Kim, Y. Chang, I. Kim, H. Lee, J. Gwack, S. Kim, M. Lim, S. Kweon, Y. Choe, O. Park and E. Jeong, "Coronavirus Disease Outbreak in Call Center, South Korea," *Emerging Infectious Diseases,* vol. 26, no. 8, pp. 1666-1670, 2020.

[35] C. Stein-Zamir, N. Abramson, H. Shoob, E. Libal, M. Bitan, T. Cardash, R. Cayam and I. Miskin, "A large COVID-19 outbreak in a high school 10 days after schools' reopening, Israel, May 2020," *Eurosurveillance,* 2020.

[36] J. Lu, J. Gu, K. Li, C. Xu, W. Su, Z. Lai, D. Zhou, C. Yu, B. Xu and Z. Yang, "COVID-19 Outbreak Associated with Air Conditioning in Restaurant, Guangzhou, China," *Emerging Infectious Diseases,* vol. 26, no. 7, pp. 1628-1631, 2020.

[37] N. C. Khanh, P. Q. Thai, H.-L. Quach, N.-A. H. Thi, P. C. Dinh, T. N. Duong, L. T. Q. Mai, N. D. Nghia, T. T. A., L. N. Quang, T. D. Quang, T.-T. Nguyen, F. Vogt and D. D. Anh, "Transmission of Severe Acute Respiratory Syndrome Coronavirus 2 During Ling Flight," *Emerging Infectious Diseases,* vol. 26, no. 11, 2020.

[38] G. Buonanno, L. Morawska and L. Stabile, "Quantitative Assessment of the Risk of Airborne Transmission of SARS-COV-2-Infection: Prospective and Retrospective Applications," *Preprint MedXRiv,* 2020.